Journal of Hazardous Materials 162 (2009) 351–355

Contents lists available at ScienceDirect

Journal of Hazardous Materials

journal homepage: www.elsevier.com/locate/jhazmat

Adsorption and aggregation of Fe(III)–hydroxy complexes during the photodegradation of phenol using the iron-added-TiO_2 combined system

Mst. Shamsun Nahar*, Kiyoshi Hasegawa, Shigehiro Kagaya, Shigeyasu Kuroda

Department of Chemical and Biochemical Engineering, Faculty of Engineering, University of Toyama, 3190 Gofuku, Toyama 930-8555, Japan

ARTICLE INFO

Article history:
Received 11 February 2008
Received in revised form 12 May 2008
Accepted 12 May 2008
Available online 21 May 2008

Keywords:
Titanium oxide
Adsorption
$Fe(OH)^{2+}$
Photocatalyst
UV light
Combined system

ABSTRACT

The behavior of Fe(III) aquacomplexes in TiO_2 suspensions in the degradation of phenol has been investigated. The most active $Fe(OH)^{2+}$ species adsorbed on the surface of TiO_2 retards the conversion of $Fe(OH)^{2+}$ into oligomers and therefore increases the percentage of $Fe(OH)^{2+}$ with irradiation time, with a consequent enhancement in the catalytic cycle of Fe(III)/Fe(II) and excited charge traps by Fe(III) in the iron–TiO_2 system. The influence of iron addition on TiO_2 was obtained when the regeneration of $[Fe(OH)^{2+}]$ remained continuous with irradiation time. In an optimum TiO_2 suspension (0.5 g/L) with the addition of 0.1 mM Fe(III), the measured k_{obs} values for phenol degradation were enhanced for the higher adsorption of $Fe(OH)^{2+}$ on the reactive surface of TiO_2 at a specified irradiation time.

© 2008 Elsevier B.V. All rights reserved.

1. Introduction

Despite its favorable photochemical efficiency, the stability of $Fe(OH)^{2+}$ is kinetically limited in aqueous media because of its rapid polymerization properties. The complexity of acidic Fe(III) solutions and their properties are well documented in the literature[1–5]. The predominant complex ionic species, monomeric $Fe[(OH)(H_2O)_5]^{2+}$ (abbreviated as $Fe(OH)^{2+}$), has been reported to possess the highest quantum yield [2,3]. The percentage of $Fe(OH)^{2+}$ ions strongly depends on the inorganic anionic ligand content [6,7], the age of the ferric solution [8], and on the starting concentration [3]. Nahar et al. [3] determined that the rate of phenol disappearance increased when the percentage of the monomeric species of Fe(III) in the solution increased. Based on acid–base thermodynamic equilibrium, the monohydroxy complex $Fe(OH)^{2+}$ would be a predominant form of Fe(III) in aqueous solution between the pH values of 3.0–4.5 [2]. However, the concentration of monomeric species rapidly decreases after the dissolution of ferric perchlorate in water and converted into less active oligomers [3,8]. Therefore, it is very important to control the aggregation of reactive $Fe(OH)^{2+}$ species with irradiation time. Degussa P25 is a very active catalyst in its mixed phase [9] and several investigators have compared the kinetics of the Fe(III)–TiO_2 combined system with the degradation rate of the pollutant [8,10–13]. To our knowledge, there are no detailed reports on the aggregation states of $Fe(OH)^{2+}$ species for various Fe(III) concentrations in the Fe(III)–TiO_2 combined system. This is the first time we have successfully investigated and applied the adsorption properties of TiO_2 with the purpose of retarding the aggregation of $Fe(OH)^{2+}$ species in the Fe(III)–TiO_2 combined system.

The main objectives of this research are to retard the polymerization of $Fe(OH)^{2+}$ species without using any electrolytes and to optimize the conditions to keep the highest concentration of reactive $Fe(OH)^{2+}$ species on the TiO_2 surface. This improved process has been used to stabilize the predominant state of $Fe(OH)^{2+}$ species during the irradiation time.

2. Experimental

2.1. Materials

Degussa P25 TiO_2 was obtained from Nippon Aerosil Co., 8-hydroxyquinoline-5-sulfonic acid was obtained from Tokyo kaseikogyo Co. Ltd. and iron(III) perchlorate $Fe(ClO_4)_3$. H_2O was obtained from Aldrich chemical company, USA. Phenol, benzene, sodium acetate, 1,10-phenanthroline, monohydrate and acetonitrile (HPLC grade) were purchased from Wako pure chemical industries Ltd.

* Corresponding author. Tel.: +81 76 445 6665; fax: +81 76 445 6549.
E-mail address: msnahar@yahoo.com (Mst.S. Nahar).

0304-3894/$ – see front matter © 2008 Elsevier B.V. All rights reserved.
doi:10.1016/j.jhazmat.2008.05.046

2.2. Apparatus

Photoirradiation was performed onto a cylindrical Pyrex reaction cell (100 mL: 50 mm i.d. × 51 mm length) with a WACOM HX-500Q [14]. For light of λ = 365 nm, Pyrex (λ > 290 nm) and Toshiba UV-35 (λ > 350 nm) cutoff filters, and a Toshiba UV-D36A band-pass filter (300 nm < λ < 380 nm) were used. The amount of light (I_0) entering the reaction cell was measured with potassium tris(oxalato)ferrate(III) actinometry. I_0 (photons mL^{-1} s^{-1}) was estimated to be 2.14×10^{15} for UV light (λ = 365 nm).

2.3. Analysis

2.3.1. Fe(III) measurement (HQSA method)

Fe(III) concentration was measured by the HQSA method, 1 mL of 0.05 mol L^{-1} 8-hydroxyquinoline-5-sulfonic acid (HQSA) and 1 mL of acetic buffer (pH 4.6) were poured into a 10 mL volumetric flask. Eight milliliters of sample was added to the solution and rapidly mixed. Within 30 s of mixing, the absorbance of the triscomplex of 8-hydroxyquinoline-5-sulfonate acid (HQS) with Fe(III), $Fe(HQS)_3$, was measured at λ = 572 with a Shimadzu UV-1600 spectrophotometer. The same mixture of HQSA and acidic buffer with 8 mL of water was used as a blank sample [15].

2.3.2. Fe(II) measurement

The Fe(II) concentration was determined by complexometry with *ortho*-phenanthroline [10].

2.3.3. Measurement of OH• radical

The concentration of •OH was monitored by following the appearance of phenol (HPLC) from the •OH mediated oxidation of added benzene [16].

2.4. Photocatalytic degradation of phenol

Titanium dioxide (P25) catalyst (0.05 gm) was added into 100 cm^3 phenol solution (100 μM) and the suspension was magnetically stirred in the dark for 30 min to reach adsorption equilibrium. After that, different concentrations (0.05, 0.1, 0.3, 0.5 mM) of iron solution ($Fe(ClO_4)_3 \cdot 6H_2O$) were added with stirring for 2 min at natural pH 3.5. The irradiation started immediately at room temperature and the remaining concentration of phenol was measured by HPLC. According to our experimental results using P25 TiO_2, the difference in k_{obs} between pH 3.0 and 4.4 is less than 5%. The natural pH value was 3.5 for the mixture of 0.1 mM Fe(III) solution in 0.5 g/L TiO_2 suspensions and this value was maintained during the entire experiment.

3. Results and discussion

3.1. Adsorption percentages of $Fe(OH)^{2+}$ species on TiO_2 surface

In this study, $Fe(ClO_4)_3$ has been selected, as it acts more efficiently in aqueous solutions containing weakly coordinating anionic ligands (ClO_4^-), and the dominant ion pair $(FeOH)^{2+}$ remains in the suspension [6,7]. The four hydrolytic speciations of Fe(III) can be represented by the following equilibrium, $Fe^{3+} + H_2O \rightarrow Fe(OH)^{2+} + H^+$ [2].

Before irradiation, the adsorption percentage of $Fe(OH)^{2+}$ was measured for Fe(III) concentrations in TiO_2 suspensions after mixing for a period of 2 min. Table 1 represents the initial percentage of $Fe(OH)^{2+}$ for various concentrations of Fe(III) salt and is correlated with the disappearance of $Fe(OH)^{2+}$ species and with the adsorption of monomeric species on TiO_2, which enabled the durability of $Fe(OH)^{2+}$ in iron–TiO_2 suspensions. The additional concentration of Fe(III) in TiO_2 (0.5 g/L) suspensions increased as follows: 0.05 mM > 0.1 mM > 0.3 mM > 0.5 mM, where the adsorption percentage of $Fe(OH)^{2+}$ was 95% > 94% > 74% > 47%, respectively. The color change of the suspensions depended on the concentration of Fe(III) and also on aging time [8]. The amount of TiO_2 (0.5 g/L) catalyst has a particular adsorption capacity for $Fe(OH)^{2+}$ species on its surface for a continuous redox reaction and the remaining $Fe(OH)^{2+}$ species in suspensions (0.3, 0.5 mM) rapidly changed to form soluble, less active aggregates or were adsorbed onto the TiO_2 surface. The color of suspensions changed from white to brown to reddish brown and this was attributed to the polymerization of $Fe(OH)^{2+}$ monomer. The adsorption percentage and the oligomerization of $Fe(OH)^{2+}$ by aging proved that the aggregation starts at 0.3 mM to concentrations above that of Fe(III) in 0.5 g/L TiO_2 suspensions.

3.2. UV–vis absorption spectra of Fe(III) solutions, with and without TiO_2

To confirm the aggregation we measured the UV–vis absorption spectra of irradiated and non-irradiated solutions using the single (0.1 mM Fe(III)) and mixed catalyst (0.1 mM Fe(III) with 0.5 g/L TiO_2) system. Aging of the reactive $Fe(OH)^{2+}$ species for Fe(III) solution caused a red shift into the visible region, as shown in Fig. 1a; this spectral change depended primarily on the formation of iron(III) aggregates and oligomers [1,8]. Spectra line D-1 shifted to D-30 for 30 min aging under dark and spectra line L-5 shifted to L-30 for 5 and 30 min irradiation time, respectively. These lines show a difference in visible absorption for irradiated solutions (L-5 to L-30), which are smaller than the difference of visible absorption of iron(III) solutions under dark conditions (D-1 to D-30), because $Fe(OH)^{2+}$ takes part in the reaction and is able to decrease the aggregation rate compared with the iron(III) solution under dark. Fig. 1b represents the spectra lines for C-1 and C-2, which are obtained for the iron–TiO_2 combined system for irradiation times of 5 and 30 min, and C-3, which is for dark conditions, where the 94% $Fe(OH)^{2+}$ was adsorbed on the TiO_2 surface before irradiation. $Fe(OH)^{2+}$ shows an absorption maximum at 295 nm for spectra lines D-1, D-30, L-5, L-30 and even for lower absorption of C-3, but there is no absorption peak at 295 nm for C-1 and C-2, as it mainly contains Fe(II). The spectra lines C-1, C-2 and C-3 give clear evidence that visible absorption has not occurred for long irradiation times, ensuring that the maximum percentage of $Fe(OH)^{2+}$ species was continuously

Table 1
Adsorption percentage of $Fe(OH)^{2+}$ species on the TiO_2 (0.05 g/l00 mL) surface for different concentration of $Fe(ClO_4)_3$ (0.05–0.5 mM) before irradiation

Fe aquacomplexes				Iron–TiO_2 suspensions, adsorption time 2 min			
$[Fe(ClO_4)_3]$ (mM)	Initial concentration (mM)		Color (30 min aging)	Remain in suspensions (mM)		Adsorption, %$Fe(OH)^{2+}$	Color (30 min aging)
	$[Fe(OH)^{2+}]$	%$Fe(OH)^{2+}$		$[Fe(OH)^{2+}]$	%$Fe(OH)^{2+}$		
0.05	0.0416	83.2	Light brown	0.0021	5.2	95.0	White
0.10	0.082	81.5	Brown	0.004	4.5	94.0	White
0.30	0.2487	82.0	Deep brown	0.0571	19	74.0	Brown
0.5 0	0.444	88.0	Reddish brown	0.2343	28.8	47.0	Deep brown

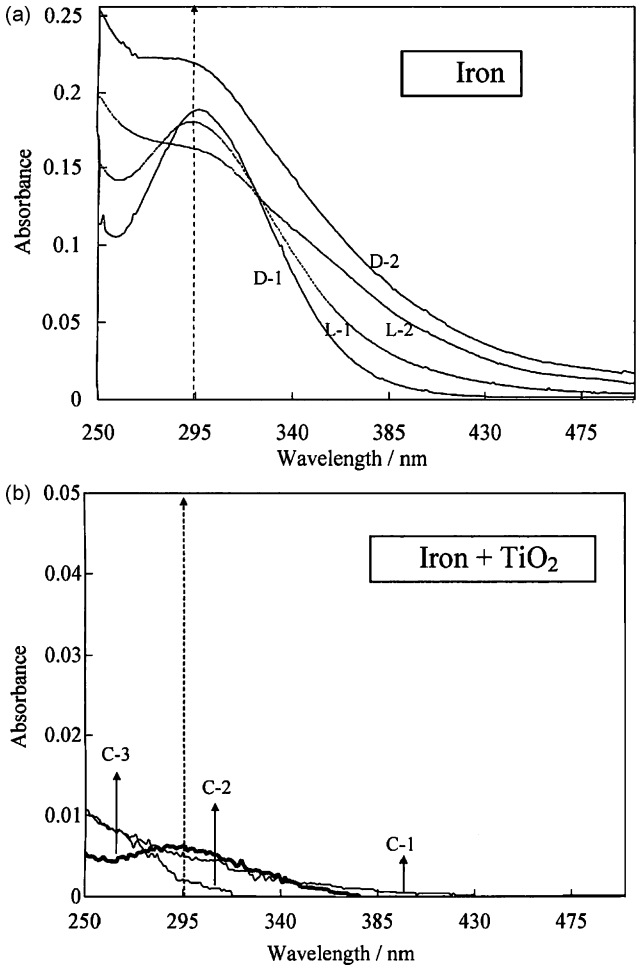

Fig. 1. (a) UV–vis absorption spectra of 0.1 mM $Fe(ClO_4)_3$ in water at natural pH aged for 30 min, D-l: aging time 1 min, D-2: aging time 30 min, L-l: irradiation 5 min, L-2: irradiation 30 min; (b) UV–vis absorption spectra of 0.1 mM $Fe(ClO_4)_3$ in TiO_2 suspensions at the time of irradiation, C-l: 5 min irradiation, C-2: 30 min irradiation, C-3: 2 min adsorption in dark.

reactive on the TiO_2 surface through the Fe(III)/Fe(II) cycle, and that oligomerization had not proceeded in the irradiated solution medium. The stability of monomeric iron species corresponds to the adsorption of $Fe(OH)^{2+}$ on the surface of TiO_2 and moreover, when $Fe(OH)^{2+}$ converts to Fe(II) by $e^-(TiO_2)$, Fe(II) dissolves into solution from the TiO_2 surface, because the reoxidation of Fe(II) by $h^+(TiO_2)$ is unlikely [17] and a new regenerated $Fe(OH)^{2+}$ species from Fe(II) with •OH will take this vacant area on the TiO_2 surface very quickly.

3.3. Influence of $Fe(OH)^{2+}$ concentration in irradiated iron aquacomplexes

Fig. 2 represents the photoirradiation rate of Fe(III) species according to the following reaction, $Fe(OH)^{2+} + h\nu \rightarrow Fe^{2+} + {}^{\bullet}OH$, and the reaction rate increases from higher concentration to lower concentration of $Fe(ClO_4)_3$ and the rate was as follows: 0.1 mM > 0.3 mM > 0.5 mM for iron alone. Here, the reaction rate for lower concentrations of Fe(III) (0.1 mM) is higher in solution.

The conversion rate of $Fe(OH)^{2+}$ to Fe(II) gradually decreases with aggregation (Fig. 1a).

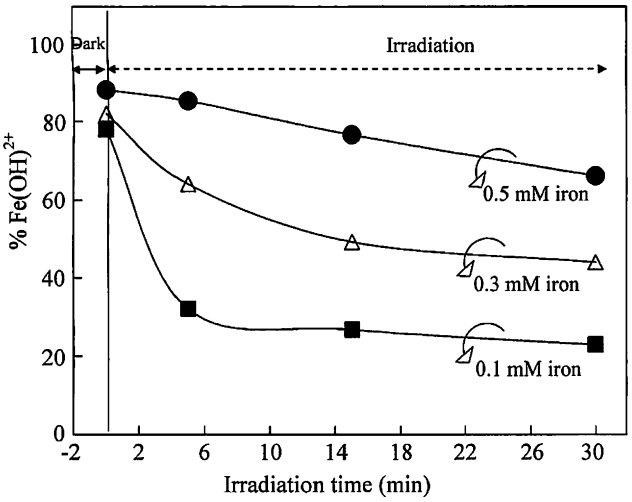

Fig. 2. The aging of the $Fe(OH)^{2+}$ for various concentration of $Fe(ClO_4)3$ under UV light irradiations: (■) $\%Fe(OH)^{2+}$, 0.1 mM $Fe(ClO_4)_3$; (△) $\%Fe(OH)^{2+}$, 0.3 mM $Fe(C1O_4)_3$; (●) $\%Fe(OH)^{2+}$, 0.5 mM $Fe(ClO_4)_3$.

3.4. Time dependence of the concentration of Fe(III) ions in suspensions of TiO_2 (0.5 g/L) with 0.1 mM of Fe(III) under dark and under UV light irradiation

Fig. 3 represents the time dependence of the Fe(II) ion concentration for two photocatalytic systems under dark and UV light irradiation conditions. Upon continuous irradiation of the combined system, the concentration of Fe(II) quickly rose within 5 min irradiation, then reached a constant value (Fig. 3, line A). After 30 min irradiation, [Fe(II)] reached a value which was (Fig. 3, line A) 4.7 times higher than without TiO_2 (Fig. 3, line B). Line B is not enhanced as is line A for lower concentrations of Fe(II) in one catalytic system (iron alone) and aggregation of $Fe(OH)^{2+}$. The adsorption of Fe(III) on the surface of TiO_2 is much higher than that of Fe(II) [17]. Therefore, Fe(III) would be rapidly reduced to Fe(II) by photoexcited electrons on the surface of TiO_2 and the reoxidation of Fe(II) to Fe(III) by holes would be reduced, due to the rapid desorption of the resultant Fe(II) ions [17]. The acceleration of Fe(II) formation (Fig. 3 line A) for 0.1 mM Fe(III), combined with TiO_2, increases the photocatalytic cycle Fe(III)/Fe(II) [10], allowing the

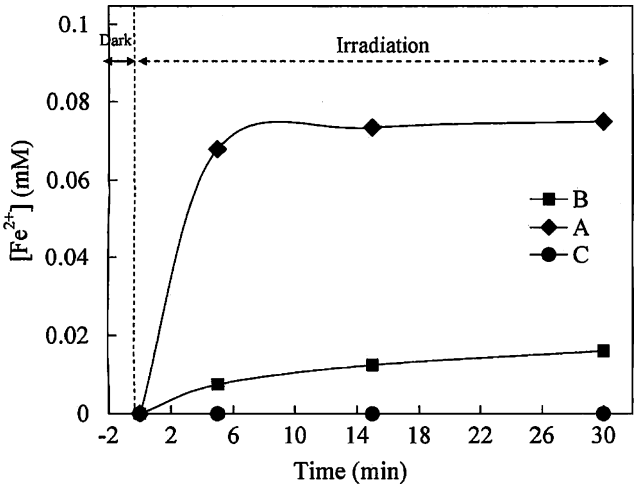

Fig. 3. Time dependence of the concentrations of Fe(II) ions fbr two catalytic systems under dark and under UV light irradiations. (♦) A: [Fe(II)], under light with TiO_2 and $Fe(C1O_4)_3$; (■) B: [Fe(II)], under light with $Fe(ClO_4)_3$; (●) C: [Fe(II)], under dark with $Fe(ClO_4)_3$.

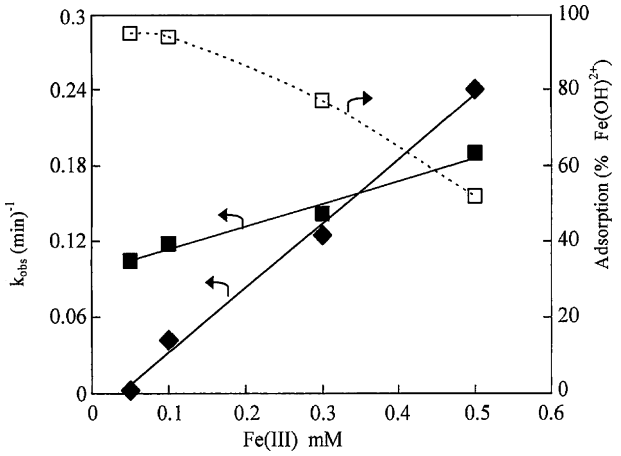

Fig. 4. Dependence of k_{obs} of the phenol degradation on various Fe(III) concentrations without TiO_2 and on adsorption percentage of $Fe(OH)^{2+}$ on TiO_2 surface under UV irradiation: (■) k^1_{obs} (TiO_2 + $Fe(ClO_4)_3$), (♦) k^2_{obs} ($Fe(ClO_4)_3$) and (□) adsorption % $Fe(OH)^{2+}$.

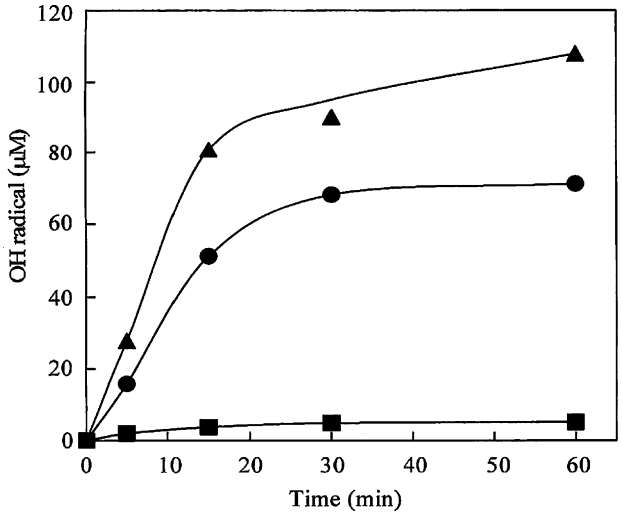

Fig. 5. Comparison of OH radical formation for three photocatalysts under UV 1ight irradiation: (■) 0.1 mM $Fe(ClO_4)_3$, (●) TiO_2 and (▲) 0.1 mM $Fe(ClO_4)_3$ + TiO_2.

continuous formation of •OH radicals. Line C shows the absence of Fe(II) in the suspensions under dark conditions.

3.5. Relation between adsorption and photoirradiation

Fig. 4 shows the relation between the adsorption of $Fe(OH)^{2+}$ and the photoirradiation of phenol by a two catalyst system. The k_{obs} values in the UV photodegradation by iron and the iron–TiO_2 combined system were plotted versus the Fe(III) concentration. An increase in the Fe(III) concentration from 0.05 to 0.5 mM significantly enhanced the degradation rate (linearly) in the absence of TiO_2, reaching a maximum value at 0.5 mM and the phenol degradation rate for 0.5 mM Fe(III) was about 96 times greater than for 0.05 mM Fe(III). The degradation rates for the heterogeneous mixture of phenol with the iron–TiO_2 system were also evaluated in Fig. 4 by the observed rate constant (k^1_{obs}). The Fe concentration in the Fe(III)–TiO_2 system is increased as 0.05 mM < 0.1 mM < 0.3 mM < 0.5 mM, and the increased adsorption concentrations of $Fe(OH)^{2+}$ species for the corresponding solutions concentration are as follows, 0.0396 mM (95%), 0.076 mM (94%), 0.1916 mM (74%), 0.209 mM (47%). On the other hand, the k^1_{obs} values increase in the order 0.104 (0.05 mM) < 0.118 (0.1 mM) < 0.142 (0.3 mM) < 0.190 (0.5 mM), respectively. Therefore, the Fe(III) concentration increases up to 10 times from lower concentration (0.05–0.5 mM), whereas the reaction rate increases only 1.8 times for 0.5 mM than for 0.05 mM under optimum TiO_2 concentrations. In the case of Fe(III) alone, the k^2_{obs} values for phenol degradation increase linearly (0.0025 < 0.05 < 0.12 < 0.24) according to the Fe(III) concentrations from 0.05 to 0.5 mM. As compared to the k^1_{obs} and k^2_{obs}, the degradation rate of phenol (Fig. 4) in the Fe(III) and Fe(III)–TiO_2 combined system is entirely dependent on increasing concentrations of $Fe(OH)^{2+}$ species by the reoxidation of higher concentrations of Fe(II) at the irradiation time (Fig. 3). The degradation rate is not dependent on the initial concentration of $Fe(OH)^{2+}$ before irradiation, but that is possible only for optimal adsorption of $Fe(OH)^{2+}$ onto TiO_2 surfaces. The decreasing activity of 0.3–0.5 mM Fe(III) in TiO_2 suspensions is related to two things, one being over adsorption of Fe(III) aquacomplexes shaded and deactivated on the reactive surface of TiO_2, and the second being the large amount of $Fe(OH)^{2+}$ remaining in the suspension which aggregates rapidly and produces less photoactive oligomers. The total degradation rate decreases for high concentrations of Fe(III) in the combined system.

3.6. Comparison of the hydroxyl radical formation from various catalysts

Three catalysts of potential interest as photocatalysts were measured in terms of their production of •OH radicals. Fig. 5 shows a comparison of the •OH formation from different catalysts under UV light irradiation. Differences in their reaction cycles produce a different amount of hydroxyl radicals and the rates are as follows: combined system > TiO_2 > $Fe(ClO_4)_3$. The amount of •OH for the combined system was 21 and 1.5 times greater than the values for $Fe(ClO_4)_3$ and TiO_2, respectively.

3.7. Reaction mechanism

The photolysis of iron alone leads to the following process:

$$Fe(OH)^{2+} + h\nu \rightarrow Fe(II) + {}^{\bullet}OH$$

$$Fe(OH)^{2+} + \text{aging} \rightarrow \text{oligomer(lessactive)}$$

$$\text{oligomer}(Fe_2(H_2O)_8(OH)_2{}^{4+}\text{dimmer} + \text{polymer}) + h\nu \rightarrow Fe(II) + {}^{\bullet}OH$$

For the iron–TiO_2 combined system, aggregation is retarded by the adsorption of $Fe(OH)^{2+}$ species on the surface of TiO_2. Fig. 6 illustrates that electrons are transferred from rutile to anatase in P25 (TiO_2) particles, which hints at a synergistic effect between rutile and anatase particles in the reaction. For mixed phases, electron and hole separation increases by rutile excitation in TiO_2 (P25). In the combined system (Fig. 6), Fe(III) reduces the recombination rate of electron and holes in TiO_2 (P25) by the following mechanism:

$$TiO_{2(Rutile)} + h\nu \rightarrow TiO_{2(rutile)}(e^- + h^+) \rightarrow e^- \rightarrow \text{interfacialarea} \rightarrow TiO_{2(anatase)}\text{surfacearea}$$

$$Fe(III) + e^-(TiO_2) \rightarrow Fe(II)$$

$$h^+(TiO_2) + OH(surf)^- \rightarrow {}^{\bullet}OH$$

$$Fe(OH)^{2+} + \text{aging} \rightarrow \text{retardthisreactionstepbyadsorption}$$

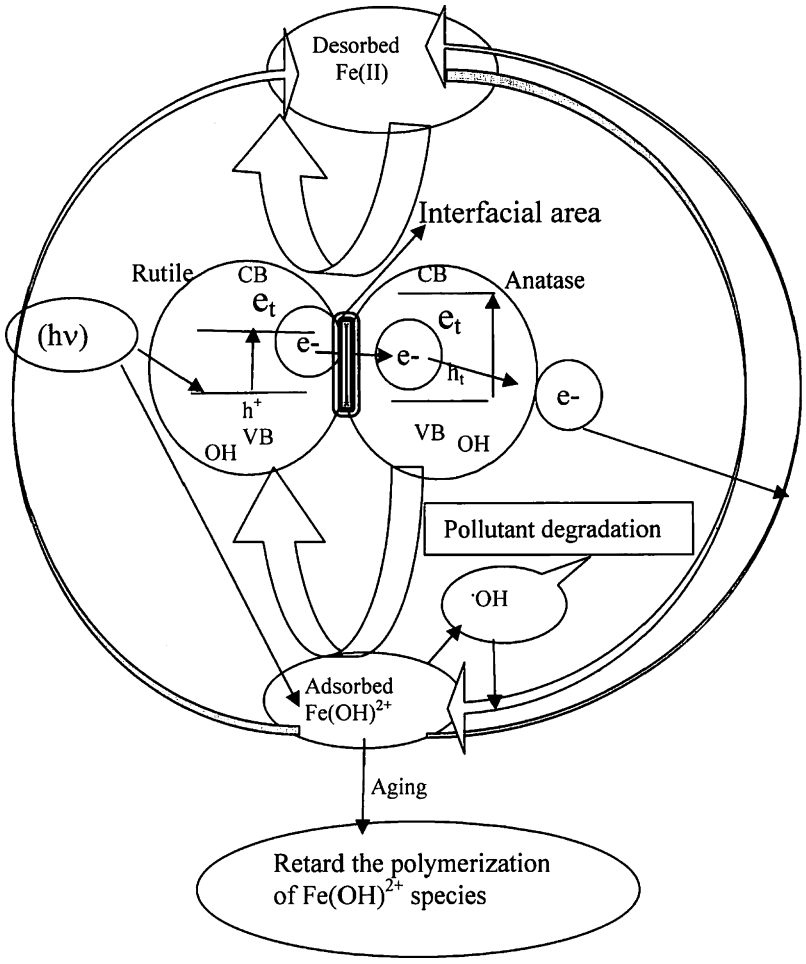

Fig. 6. Reaction cycle of iron–P25 (TiO_2) combined system.

The regeneration reaction in the suspensions can be expressed as: Fe(II) + (•OH, HO_2, H_2O_2) → Fe(III) monomer. The overall reaction represents the increasing catalytic activity influenced by one other in the combined system. The counter anions (ClO_4^-) used the •OH radical and produced the less active ClO_4• radical [18], but this effect was smaller for lower concentrations of $Fe(ClO_4)_3$.

4. Conclusions

Aggregation of Fe $(OH)^{2+}$ species was prevented by adsorption of Fe (III) onto TiO_2. On the TiO_2 surface, the Fe(III) ions are rapidly converted to Fe(II) by the photogenerated electron (e^-) of TiO_2, the recombination rate of electrons and holes is reduced, as is the •OH radical formation rate by the holes of TiO_2. Over loading Fe $(OH)^{2+}$ species shade the TiO_2 surface and also increases the aggregation percentage while decreasing the photodegradation rate for the combined system.

Acknowledgements

The research was financially supported by a grant-in-aid for Scientific Research (No. 17510063) from the Ministry of Education, Science, Sports and Culture of Japan, which is hereby gratefully acknowledged.

References

[1] R.J. Knight, R.N. Sylva, J. Inorg. Nucl. Chem. 37 (1975) 779.
[2] B.C. Faust, J. Hoigne, Atmos. Environ. 24A (1990) 79.
[3] M.S. Nahar, K. Hasegawa, S. Kagaya, S. Kuroda, Bull. Chem. Soc. Jpn. 80 (2007) 1017.
[4] H.J. Benklberg, P.J. Warneck, J. Phys. Chem. 99 (1995) 5214.
[5] V. Kabita, K. Palanivelu, Chemosphere 55 (2004) 1235.
[6] F. David, P.G. David, J. Phys. Chem. 80 (1976) 105.
[7] Z. Danna, W. Feng, D. Nansheng, Toxicol. Environ. Chem. 72 (1999) 105.
[8] C.M. Flynn, Chem. Rev. 54 (1984) 31.
[9] D.C. Hurum, A.G. Agrios, S.E. Crist, K.A. Gray, T. Rajh, M.C. Thurnauer, J. Electron Spectrosc. Relat. Phenom. 150 (2006) 155.
[10] H. Mest ankova, G. Mailhot, J. Jirkovsky, J. Krysa, M. Bolt, Appl. Catal. B: Environ. 57 (2005) 257.
[11] A. Sclafani, L. Palmisano, E. Davi, J. Photchem. Photobiol. A 56 (1991) 113.
[12] C. Dominguez, J. Garcia, M.A. Pedraz, A. Torres, M.A. Galan, Catal. Today 40 (1998) 85.
[13] E. Piera, M.I. Tegedor-Tejedor, M.E. Zorn, M.A. Anderson, Appl. Catal. B 46 (2003) 671.
[14] M.S. Nahar, K. Hasegawa, S. Kagaya, Chemosphere 65 (2006) 1976.
[15] N. Brand, G. Mailhot, M. Bolte, Environ. Sci. Technol. 32 (1998) 2715.
[16] B.C. Faust, J.M. Allen, Environ. Sci. Technol. 27 (1993) 1221.
[17] T. Ohno, D. Haga, K. Kaijaki, M. Matsumura, J. Phys. Chem. B 101 (1997) 6415.
[18] C. Hu, J.C. Yu, Z. Hao, P.K. Wong, Appl. Catal. B: Environ. 46 (2003) 35.